Electrophysiology of Cardiac Arrhythmias

15

Sei Iwai, Steven M. Markowitz, and Bruce B. Lerman

Introduction

In order to understand the pathophysiology of cardiac arrhythmias, one must have a grasp of the normal cardiac cycle, which is initiated by electrical events that precede cardiac contraction. Abnormalities in the initiation and propagation of cardiac impulses result in a variety of arrhythmias. The purpose of this chapter is to highlight the cellular mechanisms responsible for normal impulse formation and conduction and to review the clinical consequences when these mechanisms are perturbed.

Cellular Electrophysiology: The Cardiac Action Potential

The cardiac action potential consists of five phases (phases 0 through 4) that are determined by channels that allow ions to flow passively down their electrochemical gradients, as well as by a series of energy-dependent ion pumps. Ion channels are protein "tunnels" that span the cell's lipid membrane. By selectively permitting the passage of specific ions, they maintain the electrochemical cell membrane potential. Flow of a specific ion through a channel is dependent on gating of the channel as well as the electrical and chemical concentration gradients of that particular ion. Ions will flow passively down a chemical gradient if the channel is gated open and will also be drawn toward their opposite charge.

S. Iwai, MD
Division of Cardiology, Department of Medicine,
Westchester Medical Center, 100 Woods Road,
Macy Pavilion, Valhalla, NY 10595, USA

S.M. Markowitz, MD • B.B. Lerman, MD (✉)
Division of Cardiology, Department of Medicine,
Cornell University Medical Center, New York Presbyterian Hospital,
525 East 68th Street, Starr 4 Pavillion, New York, NY 10021, USA
e-mail: blerman@med.cornell.edu

Sodium (Na^+) and calcium (Ca^{2+}) channels consist of a single α-subunit that contains six hydrophobic transmembrane regions (Fig. 15.1) [1]. The voltage-gated potassium (K^+) channel consists of four identical subunits each containing a six-transmembrane-spanning unit similar to Na^+ and Ca^{2+} channels. The six transmembrane units, S1–S6, form the core of the sodium, calcium, and most potassium channels.

Na^+, K^+, Ca^{2+}, and chloride (Cl^-) are principally responsible for the membrane potential (Fig. 15.2). It is helpful to recall the equilibrium potential of these ions when considering the cardiac action potential (Table 15.1). The positive and negative values reflect the intracellular potential relative to a reference electrode. When a single type of ion channel opens, the membrane potential will approach the equilibrium potential of that ion. Thus, during diastole (phase 4), the cell membrane is impermeable to Na^+. However, K^+ diffuses freely out of the cell until the concentration gradient is balanced by the negative intracellular potential that attracts K^+. This balance represents the potassium electrochemical equilibrium potential (E_K). During phase 0, when the cell membrane is freely permeable to Na^+, the membrane potential approaches +50 mV (Fig. 15.3) [2]. Typically, more than one channel type is open at a time. The resulting membrane potential is determined by the balance of the competing currents.

Phase 0 marks the initiation of the action potential. Nodal cells are characterized by an influx of Ca^{2+}, while atrial, ventricular, and His–Purkinje cells depend on an influx of Na^+. Initiation of each cardiac cycle is dependent on membrane depolarization initiated at the sinus node. In nodal cells, the pacemaker current, I_f, initiates each cycle. I_f is activated by the polarization of phase 4 and carries a nonselective inward current composed primarily of Na^+ and K^+ ions, as well as a small Ca^{2+} current. I_f causes slow depolarization of the nodal cell membranes during diastole until a threshold for firing is achieved. Following initial local membrane depolarization by I_f, the upstroke of the nodal action potential is completed by a slow inward calcium current. Two types of calcium

C. Rosendorff (ed.), *Essential Cardiology*,
DOI 10.1007/978-1-4614-6705-2_15, © Springer Science+Business Media New York 2013

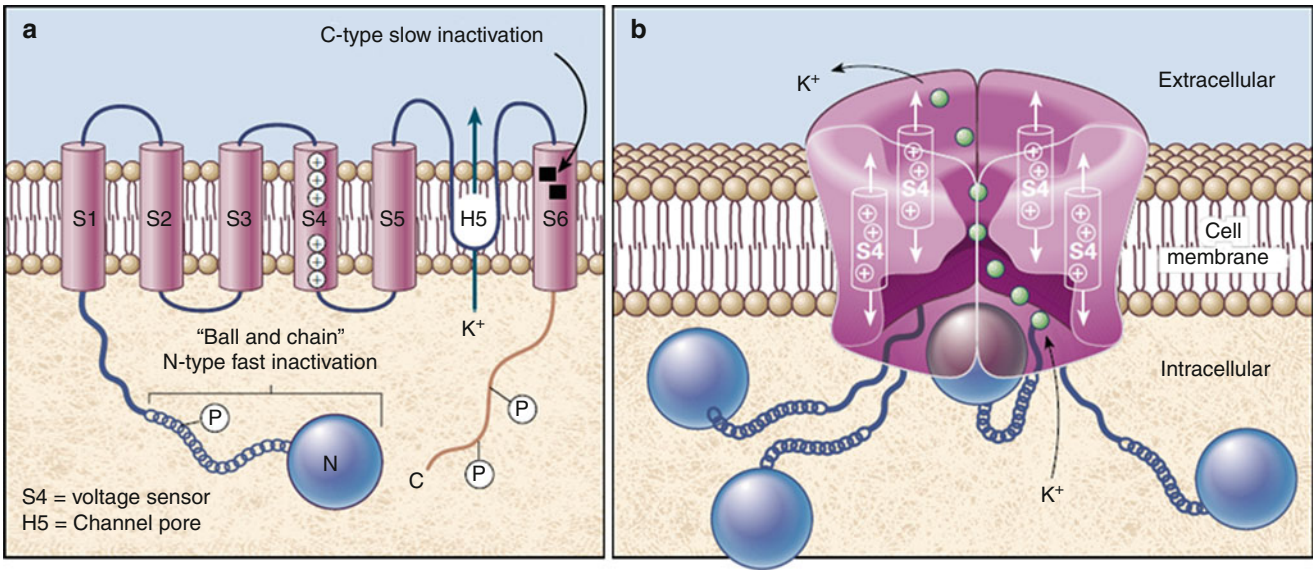

Fig. 15.1 (**a**) Diagram of a subunit containing six transmembrane-spanning motifs, S1 through S6, that forms the core structure of sodium, calcium, and potassium channels. The "ball and chain" structure at the N-terminal of the protein is the region of a potassium channel that participates in N-type "fast inactivation," occluding the permeation pathway. The *circles* containing plus signs in S4, the voltage sensor, are positively charged lysine and arginine residues. Key residues lining the channel pore (H5) are found between S5 and S6. (**b**). Diagram of the four identical subunits of the voltage-gated postassium channel, each containing a six-transmembrane-spanning unit. (Modified from Ackerman and Clapham [1]. With permission from Massachusetts Medical Society)

currents are present: the predominant slowly inactivating, dihydropyridine-sensitive L current (I_{Ca-L}) and the rapidly inactivating T current (I_{Ca-T}; *see* Fig. 15.3 and Table 15.1). Local membrane depolarization is propagated to neighboring cells via gap junction channels.

In "nonpacemaker" tissue, I_f is absent. In these cells, phase 0 is triggered when the cell membrane is depolarized by adjacent cells. Once a sufficient proportion of a cell surface is depolarized and the cell reaches its activation threshold, the permeability of the cell surface membrane to I_{Na} is markedly increased, allowing Na^+ to enter the cell and complete phase 0 depolarization. Blocking this inward current decreases the rate of change of the upstroke of the action potential (dV/dt) and slows conduction velocity.

Phase 1 consists of rapid membrane repolarization. This is achieved by inactivation of the inward Na^+ current and activation of the transient outward current (I_{to}), which is comprised of two currents. I_{to1} is a voltage-activated outward potassium current, and I_{to2} is a calcium-activated chloride current. Phase 2, the plateau phase, may last as long as 100 ms and is characterized by a small change in membrane potential generated by I_{Ca-L}.

Rapid repolarization of the cell occurs during phase 3. I_{Ca-L} is inactivated in a time-dependent fashion, thus decreasing the flow of cations into the cell. Simultaneously, several outward potassium currents, known as the delayed slow (I_{Ks}), rapid (I_{Kr}), and ultrarapid (I_{Kur}) currents, become active. This results in a net outward positive current and a negative transmembrane potential.

Mechanisms of Arrhythmias

Automaticity

Rhythmic (pacemaker) activity is an inherent property of different cell types. There is a normal hierarchy in the frequency of the initiated action potentials, with the sinus node being the dominant pacemaker. Automaticity in the distal conduction system (or working myocardium) may compete with that in the sinus node on the basis of *enhanced normal* or *abnormal* automaticity.

Under pathologic conditions, a decrease in the resting membrane potential may occur, which can lead to spontaneous phase 4 depolarization in all cardiac cells [3]. Abnormal automaticity is defined as spontaneous impulse initiation in cells that are not fully polarized. The disturbances in the normal ionic balance leading to abnormal automaticity may result from perturbations in various currents, e.g., reduction in the inward rectifying current, I_{K1}. During the subacute phase (24–72 h) following coronary occlusion, automatic arrhythmias can arise from the borders of the infarction.

Clinical Correlates

A representative clinical example of an automatic arrhythmia is atrial or ventricular tachycardia that is precipitated by exercise in patients without structural heart disease. These forms of tachycardia are thought to represent adrenergically mediated automaticity, because programmed stimulation can

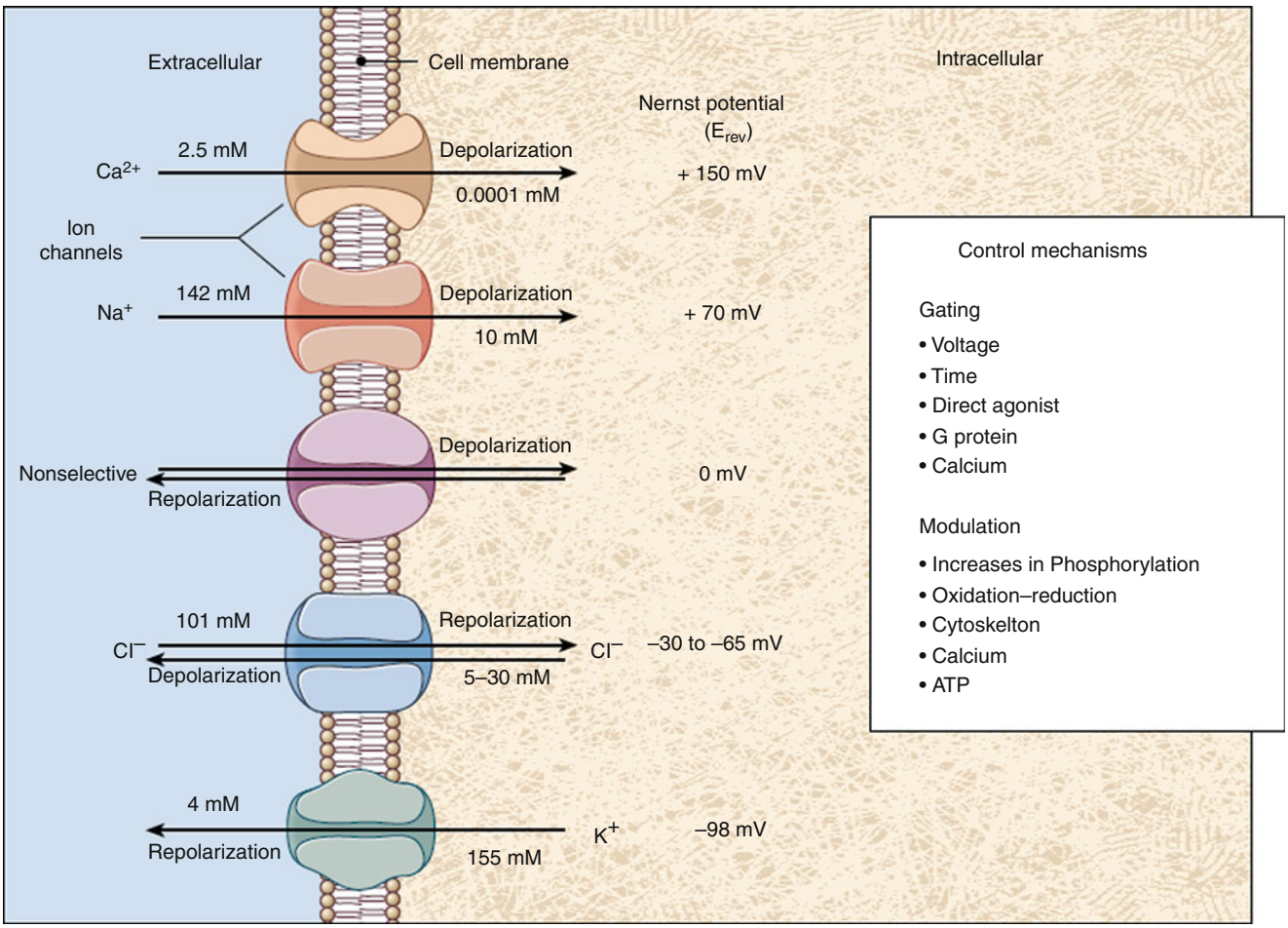

Fig. 15.2 Physiology of ion channels. Five major types of ion channels determine the transmembrane potential of a cell. The ionic gradients across the membrane establish the Nernst potentials (E_{rev}) of the ion-selective channels (approximate values are shown). Under physiologic conditions, calcium and sodium ions flow into the cell and *depolarize* the membrane potential (i.e., they drive the potential toward the values shown for E_{Ca} and E_{Na}), whereas potassium ions flow outward to *repolarize* the cell toward E_K. Nonselective channels and chloride channels drive the potential to intermediate voltages (0 mV and −30 to −65 mV, respectively) (Modified from Ackerman and Clapham [1]. With permission from Massachusetts Medical Society)

neither initiate nor terminate the arrhythmia, whereas the tachycardia can be induced with catecholamine stimulation and is sensitive to β-blockade (Table 15.2) [4, 5].

The cellular mechanism governing automatic arrhythmias and their anatomic substrate is poorly delineated. Catecholamines modulate the rate in automatic cells by increasing cyclic AMP (cAMP) synthesis and alter the kinetics of I_f such that it is activated at less negative membrane potentials [6]. Adenosine appears to attenuate I_f through an inhibition of cAMP synthesis, an antiadrenergic mechanism similar to that mediated by vagal stimulation [7].

Triggered Activity

In cardiac cells, oscillations of membrane potential that occur during or after the action potential are referred to as *afterdepolarizations*. They are generally divided into two subtypes: early and delayed afterdepolarizations (EADs and DADs, respectively; Fig. 15.4). When an afterdepolarization achieves sufficient amplitude and the threshold potential is reached, a new action potential is evoked; this is known as a triggered response. Under appropriate circumstances, this process may become iterative, resulting in a sustained triggered arrhythmia. Triggered activity differs fundamentally from abnormal automaticity in that abnormal automaticity occurs during phase 4 of the action potential and it depends on partial depolarization of the resting membrane potential.

Early Afterdepolarizations and Arrhythmogenesis

An EAD can appear during the plateau phase (phase 2) and/or repolarization (phase 3) of the action potential (Fig. 15.4). Distinction between phase 2 and phase 3 EADs is often based on the takeoff potential of the EAD, e.g., above −35 mV for the phase 2 and below −35 mV for the phase 3 EADs. It is

Table 15.1 Summary of transmembrane currents

Ion (Nernst potential)	Currents	Role in AP
Potassium (−98 mV)	I_f—inward "pacemaker" current (also carried by Na^+)	Activated in nodal tissue polarization of membrane during phase 4
	I_{K1}—inward rectifier responsible for resting membrane potential	Maintains phase 4 resting membrane potential; absent in sinus node
	I_{Kur}—inward ultrarapid rectifier	Minor current of phase 1 repolarization
	I_{Kr}—inward rapid rectifier repolarization	Primary current of rapid phase 3
	I_{Ks}—inward slow rectifier	Contributes to late phase 3 repolarization
	I_{to1} (=I_{Kto1})—transient voltage-sensitive outward current	Activated (by voltage) briefly during phase 1 rapid repolarization
	$I_{K(ACh)}$—outward current	Activated by muscarinic (M_2) receptors via GTP; important in nodal and atrial cells where it may cause hyperpolarization and shortening of action potential duration
	$I_{K(Ado)}$—outward current	Appears identical in function to $I_{K(ACh)}$, but activated by adenosine
	$I_{K(ATP)}$—outward current	Blocked by ATP; activated during hypoxia (when ATP concentration low); shortens action potential during ischemia
Sodium (+70 mV)	I_{Na}—fast inward current carried by Na^+ through a voltage-gated channel	Phase 0
	I_{Ti}—transient inward current	Activated during phase 4 by release of Ca^{2+} from the sarcoplasmic reticulum; contributes to DADs
	$I_{Na\text{-}K\ pump}$—bidirectional current	Pumps 3 Na^+ out for 2 K^+ in producing small rectifier current; when this channel is blocked by digoxin, the Na/Ca exchanger $I_{Na/Ca}$ takes over, resulting in intracellular Ca^{2+} overload
	$I_{Na/Ca}$—outward current	Exchanges 1 Ca^{2+} (into the cell) for 1 Na^+ (out of the cell) during intracellular Na^+ overload; during digoxin toxicity, this may result in intracellular Ca^{2+} overload and triggered arrhythmias
Calcium (+150 mV)	I_{Ca-L}—slow inward calcium current, blocked by dihydro-pyridines	Active during phase 0 in nodal cells, phase 2 of atrial, ventricular, and His–Purkinje cells
	I_{Ca-T}—transient inward current	May contribute to phase 4 depolarization in sinus and His–Purkinje cells
	$I_{Na/Ca}$—inward current	Exchanges 1 Ca^{2+} (out of the cell) for 3 Na^+ (into the cell) during phase 2; during digoxin toxicity, this may result in intracellular Ca^{2+} overload and triggered arrhythmias
Chloride (−30 mV)	I_{Cl}—outward current	Contributes to phase 3 repolarization; activated by adrenergic stimulation
	I_{to2} (= $I_{Cl.Ca}$)—transient (Ca^{2+} activated) outward chloride current	Activated briefly during phase 1 rapid repolarization

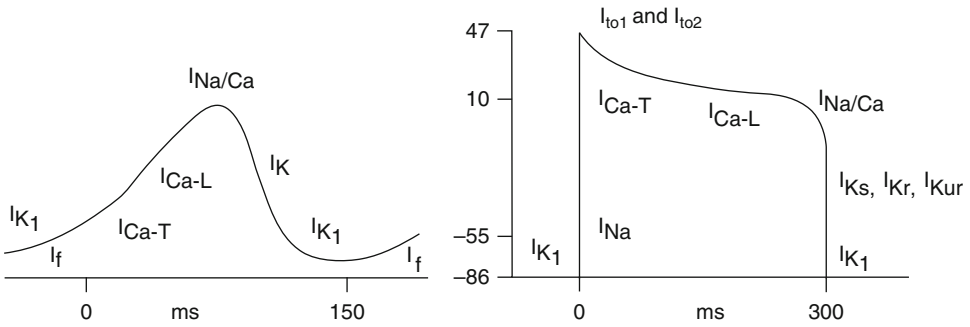

Fig. 15.3 The human cardiac action potential. Principal currents responsible for the sinoatrial nodal (*left*) and ventricular (*right*) action potential (Modified from Ackerman and Clapham [2], pp. 81–301. With permission from Elsevier)

possible for both forms of EADs to appear during the same action potential. A critical prolongation of repolarization, either by a reduction in outward currents, an increase in inward currents, or a combination of the two, is normally required for the manifestation of EAD-induced ectopic activity. EADs are often potentiated by bradycardia or a pause, which further prolongs repolarization, since action potential duration is dependent on the prior diastolic interval.

Clinical Correlates

A wide variety of medications can produce EADs, EAD-related triggered activity, or even a form of polymorphic ventricular tachycardia known as *torsade de pointes* (Fig. 15.5). These agents excessively prolong repolarization and include the Vaughan-Williams class Ia (e.g., quinidine and procainamide) and class III (e.g., sotalol, dofetilide, and ibutilide)

Table 15.2 Electropharmacologic matrix

	Reentry	Automaticity	cAMP-triggered activity
Catecholamine stimulation	Facilitates/no effect	Facilitates	Facilitates
Induction with rapid pacing	Facilitates/no effect	No effect	Facilitates
Overdrive pacing	Terminates/accelerates	Transiently suppresses	Terminates/accelerates
β-blockade	No effect/rarely terminates	Terminates	Terminates
Vagal maneuvers	No effect	Transiently suppresses	Terminates
Calcium channel blockade	No effect[a]	No effect	Terminates
Adenosine	No effect	Transiently suppresses	Terminates

Reprinted from Lerman et al. [4]. With permission from John Wiley & Sons Inc.
Automaticity refers to arrhythmias that arise from spontaneous phase 4 depolarization from nearly fully repolarized cells. Abnormal automaticity (which occurs in cells with resting membrane potentials ≤−60 mV) is not included in this table because it has not conclusively been shown to be a cause of clinical arrhythmias
[a]An exception is intrafascicular reentry, which is sensitive to verapamil

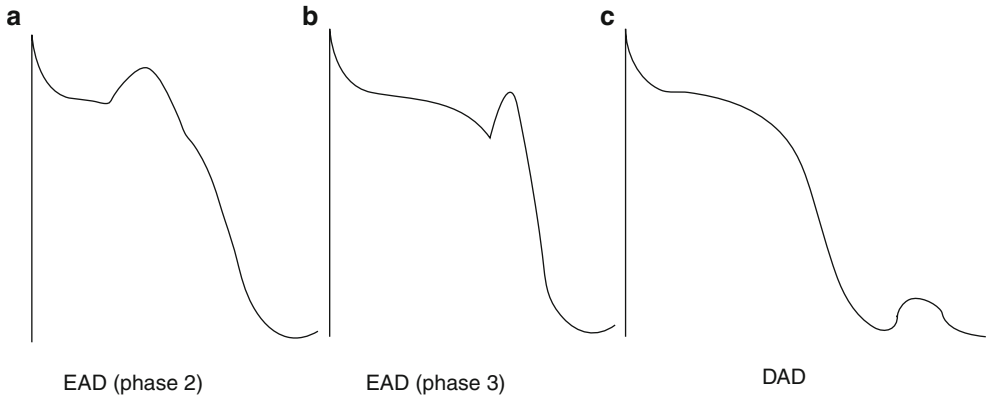

Fig. 15.4 Schematic examples of (**a**) phase 2 early afterdepolarization (*EAD*), (**b**) phase 3 *EAD*, and (**c**) delayed afterdepolarization (*DAD*)

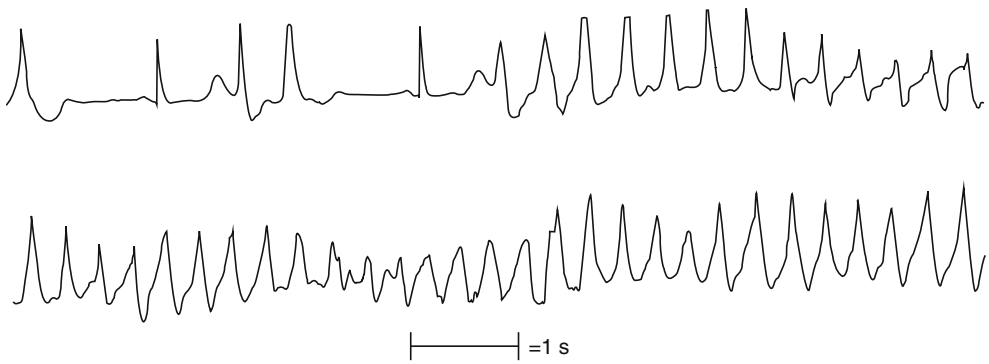

Fig. 15.5 Initiation of torsade de pointes following a "long-short" interval in a patient with long-QT syndrome

antiarrhythmic agents, and a variety of noncardiac drugs, including antibiotics (e.g., erythromycin), pentamidine, and nonsedating antihistamines (e.g., terfenadine and astemizole).

One of the most extensively studied EAD-related arrhythmias is that found in patients with congenital long-QT syndrome (LQTS). Initially thought to be a rare disease (1 per 10,000 births), more recent estimates demonstrate a much higher prevalence (1 per 2,500 births) [8]. LQTS provides an opportunity to examine the effects of ion-channel mutations on structure and function of these channels.

Two distinct phenotypes of congenital long-QT syndrome were initially recognized. In 1957 Jervell and Lange-Nielsen described the autosomal recessive pattern of the congenital long-QT syndrome associated with congenital sensorineural hearing loss and recurrent syncope [9], and in 1963, an autosomal dominant form of the disease manifesting only as QT prolongation was described separately by Romano et al. and Ward [10, 11]. Genotyping has now revealed 13 disease-causing genes for the long-QT syndrome [12].

Certain clinical features appear to be common to most forms of the congenital long-QT syndrome. Most patients will have a corrected QT interval (QTc) of 460 ms or greater [13], although some LQTS patients can have a normal QTc. The standard heart rate correction, according to Bazett's formula, is $QTc = QT/RR^{1/2}$, where RR is the R–R interval expressed in seconds. Initially, a scoring system was developed and was used to assist in the diagnosis of the long-QT syndrome and took into account factors including the QT interval, patient

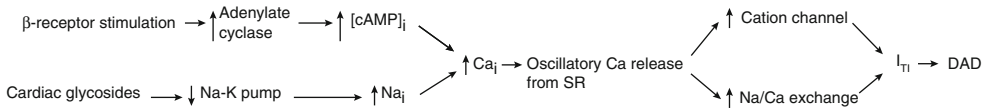

Fig. 15.6 Mechanism of DADs related to catecholamines and digoxin toxicity. Intracellular Ca^{2+} overload triggers I_{Ti}, a depolarizing inward Na^+ current. Ca_i inward Ca^{2+} current, Na_i increased intracellular Na^+ concentration, I_{TI} depolarizing inward Na^+ current, *SR* sarcoplasmic reticulum

symptoms, and family history [14]. The syndrome appears to be equally distributed between men and women.

Genetic testing for LQTS is currently available and is recommended for any patient in whom there is a strong clinical index of suspicion for LQTS (based on clinical history, family history, electrocardiogram, and/or provocative stress testing) or for any asymptomatic patient with QT prolongation in the absence of other clinical conditions that might prolong the QT interval. Furthermore, mutation-specific genetic testing is recommended for family members (and other appropriate relatives) following identification of the LQTS-causing mutation in an index case [15]. Known mutations account for about 75 % of those diagnosed with LQTS. LQT1 accounts for approximately 30–35 % of LQTS cases. The responsible gene is located on the short arm of chromosome 11 and encodes the pore forming the α-subunit (one of the two proteins) that comprise $I_{Ks,}$ the slowly activating delayed rectifier current. The defective I_{Ks} is inactive, thus prolonging repolarization and predisposing to EADs.

Mutations in the gene encoding I_{Kr} (HERG) on chromosome 7, which result in prolonged phase 3 repolarization, appear to be responsible for another autosomal recessive form of the long-QT syndrome, LQT2, and account for another 25–40 % of LQTS patients.

LQT3 has been linked to SCN5A, a gene on chromosome 3 that encodes $I_{Na,}$ the current responsible for phase 0 rapid depolarization. LQT3 results from a sodium channel that fails to inactivate appropriately and is present in 5–10 % of LQTS cases. This mutation causes continued inward sodium current (beyond phase 0) throughout the action potential, thereby prolonging the action potential duration. Mexiletine, a selective Na^+ channel blocker, has been demonstrated to shorten the QTc in affected patients and may therefore have a therapeutic role.

Less common mutations include LQT4 (ankyrin B), located on chromosome 4, which causes disruption in the cellular organization of the Na^+ pump, the Na^+/Ca^{2+} exchanger, and the inositol triphosphate receptor; extrasystoles are caused by altered Ca^{2+} signaling. In addition, the β-subunit of I_{Ks} and I_{Kr} are encoded by KCNE1 and KCNE2 (both on chromosome 21), and mutations in these genes can also result in prolonged QTc due to delayed repolarization (LQT5 and LQT6, respectively). LQT7 is caused by the mutant gene KCNJ2, which decreases the inwardly rectifying K^+ current ($I_{Kir2.1}$).

Mutations in one allele of either the α- or β-subunit of I_{Ks} appear to be phenotypically expressed as the Romano–Ward syndrome. Both subunits have been demonstrated to be present in the stria vascularis of the inner ear in mice. Mutations in both alleles (i.e., homozygotes) for the α- or β-subunit are associated with the Jervell and Lange-Nielsen phenotype.

Delayed Afterdepolarizations and Arrhythmogenesis

Delayed afterdepolarizations (DADs) are oscillations in membrane potential that occur after repolarization and during phase 4 of the action potential. In contrast to automatic rhythms that originate de novo during spontaneous diastolic depolarization, DADs are dependent on the preceding action potential. By definition, they do not occur in the absence of a previous action potential.

During the plateau phase of the normal action potential, Ca^{2+} enters the cell. The increase in intracellular Ca^{2+} triggers release of Ca^{2+} from the sarcoplasmic reticulum (SR); this, in turn, further elevates intracellular calcium and initiates contraction. Relaxation occurs through sequestration of Ca^{2+} by the SR. DADs arise when the cytosol becomes overloaded with Ca^{2+} and triggers I_{Ti}, a transient inward current (Fig. 15.6). I_{Ti} is generated by the Na^+–Ca^{2+} exchanger (I_{NaCa}) and/or a nonspecific Ca^{2+}-activated current [16, 17]. DADs can originate from Purkinje fibers, as well as from myocardial, mitral valve, and coronary sinus tissues. Rapid pacing potentiates DADs because more Na^+ (and Ca^{2+}) enters the cell during rapid depolarization, further loading the cell with Ca^{2+}. Most experimental studies on triggered activity were performed under conditions of digoxin excess. By blocking the Na^+/K^+ pump, digoxin causes increased concentration of intracellular Na^+. The high concentration of Na^+ stimulates the electrogenic Na^+/Ca^{2+} exchanger, which moves Na^+ out of the cell in exchange for allowing Ca^{2+} entry into the cytosol. This results in intracellular Ca^{2+} overload and DADs. β-adrenergic stimulation, the effects of which are mediated by an increase in intracellular cAMP, also provokes delayed afterdepolarizations by increasing the inward Ca^{2+} current.

Clinical Correlates

The prototypical clinical arrhythmia due to cAMP-mediated triggered activity (DAD dependent) is idiopathic ventricular tachycardia arising from the right ventricular outflow tract

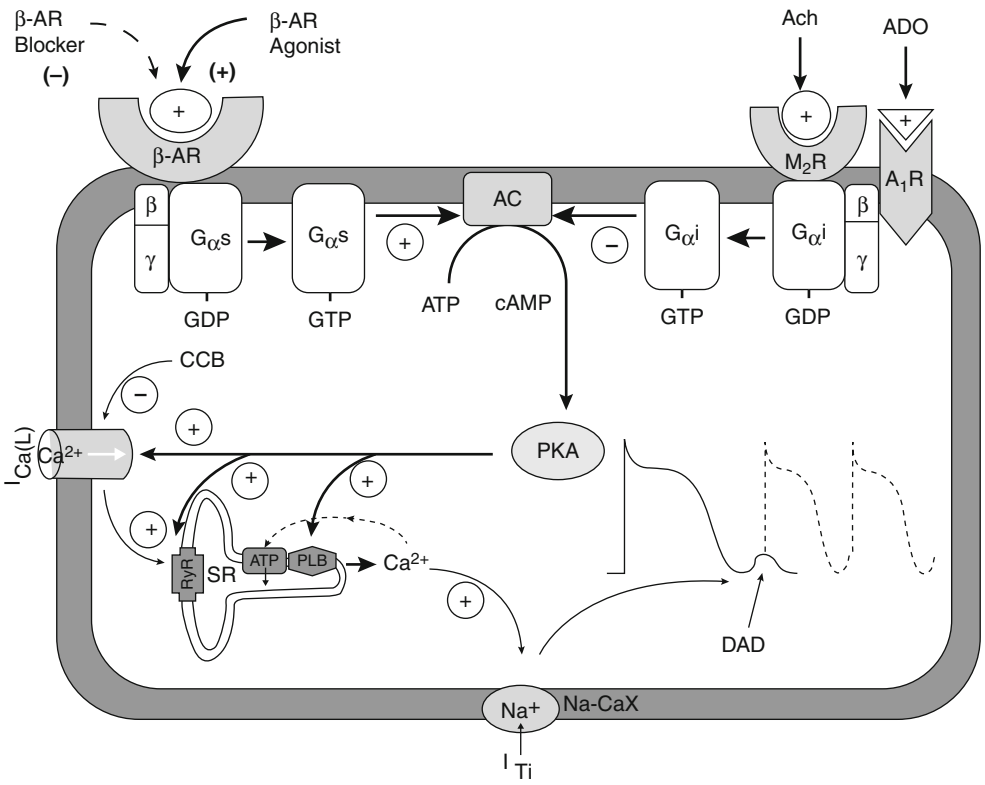

Fig. 15.7 Schematic representation of the cellular model for adenosine. *AC* adenylyl cyclase, *ACh* acetylcholine, *ADO* adenosine, A_1R adenosine A_1 receptor, *ATP* adenosine triphosphate, *β-AR* β-adrenergic receptor, *DAD* delayed afterdepolarization, $G\alpha_i$ inhibitory G protein, $G\alpha_s$ stimulatory G protein, *GDP* guanosine diphosphate, *GTP* guanosine triphosphate, M_2R muscarinic cholinergic receptor, *PKA* protein kinase A, *PLB* phospholamban, *RyR* ryanodine receptor, *SR* sarcoplasmic reticulum, *cAMP* cyclic adenosine monophosphate, I_{Ti} Transient inward current, *CCB* calcium channel blocker

(RVOT) [18] and is usually characterized by paroxysmal stress-induced VT or repetitive monomorphic VT (RMVT) [19, 20]. RMVT occurs during rest and is characterized by frequent ventricular extrasystoles, ventricular couplets, and salvos of nonsustained VT with intervening sinus rhythm. In contrast, paroxysmal stress-induced VT usually occurs during exercise or emotional stress and is a sustained arrhythmia. Common to both groups are the absence of structural heart disease, similar tachycardia morphology (left bundle branch block, inferior axis), and similar site of origin (RVOT), although the tachycardia can occasionally originate from other right ventricular sites as well as the left ventricle, especially from near the left and right coronary cusps of the sinuses of Valsalva [20, 21]. Overlap between these phenotypes of VT can be considerable.

Since activation of adenylyl cyclase and $I_{Ca–L}$ is critical for the development of cAMP-mediated triggered activity, the triggered arrhythmia would be expected to be sensitive to many electrical and pharmacological stimuli, including β-blockade, calcium channel blockade (verapamil), vagal maneuvers, and adenosine (Table 15.2; Fig. 15.7). Termination of VT with adenosine is thought to be a specific response for identifying cAMP-mediated triggered activity due to DADs, since adenosine has no ventricular electrophysiologic effect in the absence of β-adrenergic stimulation and has no effect on digoxin-induced DADs or quinidine-induced EADs. Furthermore, adenosine has no effect on catecholamine-facilitated reentry that is due to structural heart disease [22]. The clinical effects of adenosine and verapamil in a patient with VT attributed to cAMP-mediated triggered activity are shown in Fig. 15.8 [19]. While calcium blockers may be helpful in the cardiac electrophysiology laboratory in determining the mechanism of a specific arrhythmia (Table 15.2), their use is *contraindicated* in the treatment of most clinical forms of ventricular tachycardia.

Another arrhythmia that is likely due to triggered activity and delayed afterdepolarizations is *catecholaminergic polymorphic ventricular tachycardia* (CPVT). CPVT also occurs in patients with no evidence of structural heart disease, who present with a distinctive pattern of stress-related, bidirectional VT, or polymorphic VT. Mutations in the cardiac ryanodine receptor gene (RyR2) and calsequestrin 2 have been linked to CPVT [23–25]. RyR2 is responsible for calcium release from the sarcoplasmic reticulum, in response to calcium entry from the voltage-dependent L-type calcium channels (i.e., calcium-induced calcium release). Calsequestrin provides a calcium reservoir in the sarcoplasmic reticulum and possibly serves as a luminal Ca^{2+} sensor for the ryanodine receptor. Malfunction in either of these genes can result in intracellular calcium overload.

Reentry

The normal cardiac impulse follows a predetermined path. It is initiated at the sinus node and is extinguished after it has

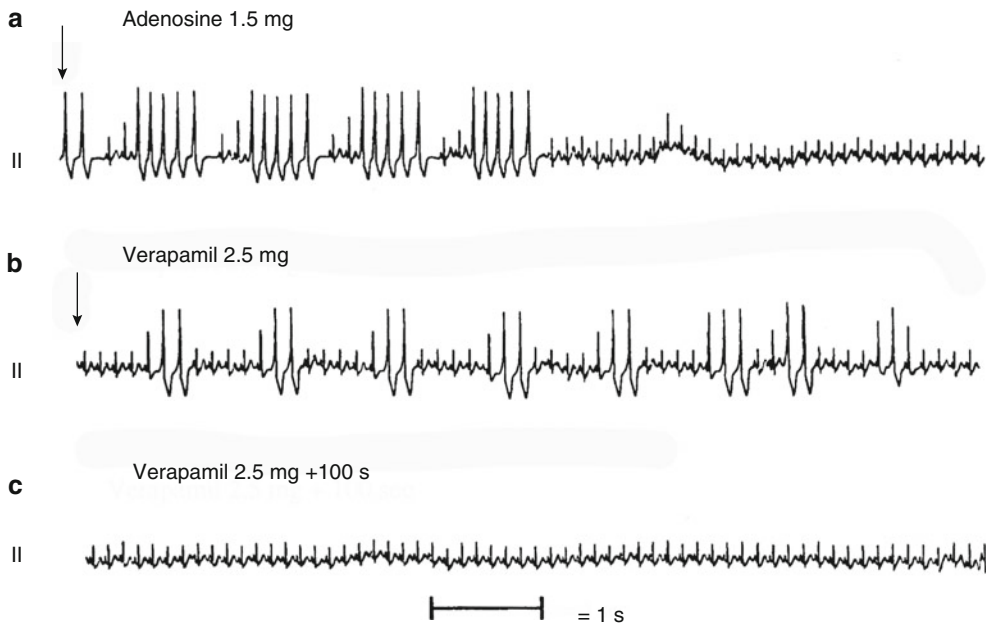

Fig. 15.8 (**a**) ECG recording showing termination of incessant repetitive monomorphic ventricular tachycardia (VT) by adenosine. The *vertical arrow* indicates the completion of adenosine administration and saline flush. (**b**) Administration of verapamil during incessant repetitive monomorphic VT. *Vertical arrow* indicates completion of verapamil infusion. (**c**) Termination of VT 100 s after verapamil administration. Surface lead II is shown (Reprinted from Lerman et al. [19]. With permission from Lippincott Williams & Wilkins)

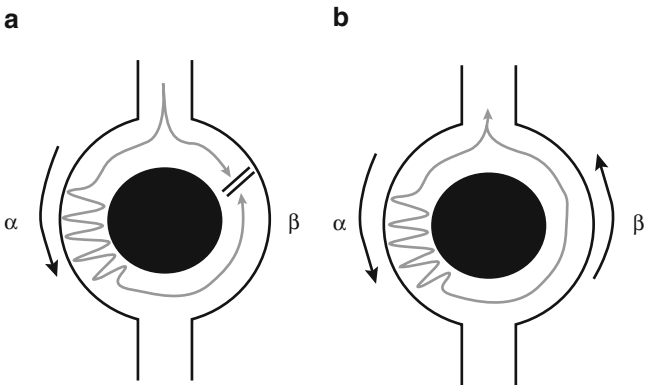

Fig. 15.9 Model of anatomic reentry. The impulse passes through a hypothetical conduit via two pathways, α and β, which meet at a common exit point. (**a**) Since α and β have distinct refractory properties, a hypothetical extrastimulus could be blocked in β pathway and conduct slowly over α pathway and reenter β pathway retrogradely. (**b**) This could result in sustained circus movement (reentry)

activated the ventricles. Reentrant arrhythmias arise when the cardiac impulse circulates around an anatomic or functional obstacle initiating an independent, repetitive rhythm. Reentry may be broadly classified as being either *anatomic* or *functional*.

Anatomic Reentry

In the anatomic model of reentrant arrhythmias, four prerequisites must be met to initiate reentry (Fig. 15.9): (1) a predetermined anatomic circuit must exist; (2) unidirectional block (e.g., in response to an extrastimulus) must occur in one limb of the reentrant circuit; (3) slow conduction in a contiguous pathway of the circuit, allowing recovery of excitability of the previously refractory limb; and (4) the wavelength of the impulse must be shorter than the length of the circuit [26, 27]. An illustration of some of these principles is shown in Fig. 15.9a, where an impulse "blocks" in the β pathway and travels down the α pathway slowly, but not with sufficient delay to allow resolution of refractoriness in the β pathway. Therefore, the retrograde impulse is extinguished. In Fig. 15.9b, conduction proceeds anterogradely down the α pathway and then subsequently retrogradely up the β pathway, which is no longer refractory. This results in reentry.

The concept of wavelength is inherent in the anatomical model of reentry. The leading edge of the wave must encounter excitable tissue in which to propagate. Therefore, the rotation *time* around the reentrant circuit must be longer than the recovery period of all segments of the circuit, and the *length* of the circuit must exceed the product of the conduction velocity and the recovery period of the tissue (Fig. 15.10a). Interruption of the anatomical circuit at any point interrupts reentry.

Functional Reentry

The mechanism of many atrial or ventricular reentrant arrhythmias may be more complex than just anatomical reentry. It has become apparent that reentry may be sustained even in the absence of a specific anatomical circuit and in the absence of abnormal myocardium. This type of reentry is termed *functional*.

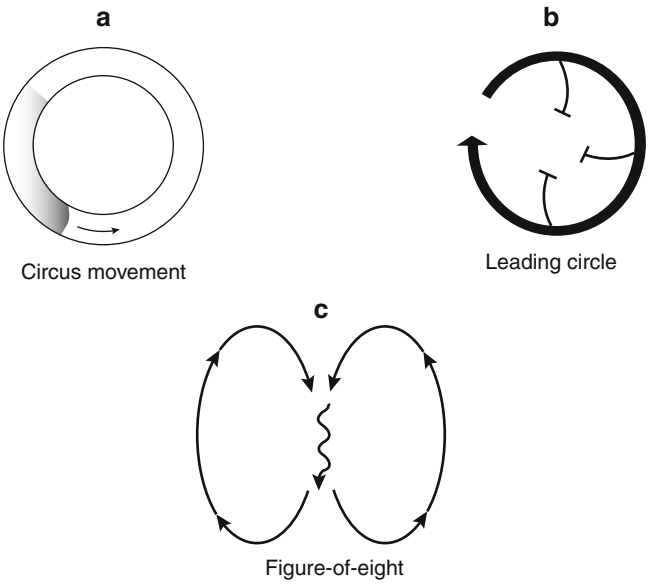

Fig. 15.10 (**a**) Circus movement reentry. The impulse (*gray region*) must be shorter than the entire length of the circuit (*circle*) and travel at a rate slow enough to allow separation of the impulse from its own refractory tail. This interval (depicted as *white*) is called the excitable gap. Reentry will be extinguished if the leading edge of the impulse (*black*) impinges on its tail (*gray*). (**b**) Model of leading circle reentry. Reentry follows the smallest possible circuit with tissue at the vortex remaining unexcitable. No anatomical barrier is present. (**c**) Figure-eight reentry in anisotropic cardiac muscle. Two reentrant circuits rotate in opposite directions sharing a central common pathway

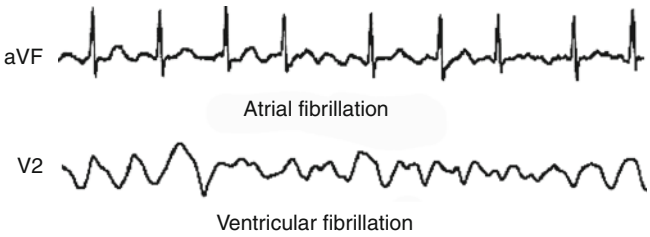

Fig. 15.11 Atrial fibrillation and ventricular fibrillation are examples of clinical arrhythmias that can be caused by spiral wave reentry

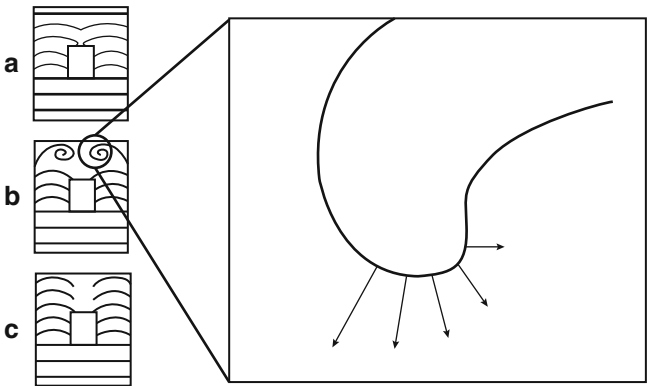

Fig. 15.12 Spiral wave reentry. (**a**) At normal levels of excitability, the wave separates into two daughter waves that circumnavigate the borders of the obstacle and fuse again at the opposite side. No wave break occurs. (**b**) At lower levels of excitability, the broken wave front curves and initiates a pair of counter-rotating spiral waves. The inset depicts propagation velocity along the curved wave front of a spiral wave. The more pronounced the curvature, the slower the conduction velocity (*small arrows*). Toward the periphery, conduction velocity reaches the maximum (*large arrows*). (**c**) Finally, at lower levels of excitability, the broken wave fronts are unable to rotate, propagating decrementally until they disappear (Reprinted from Jalife et al. [26]. With permission from John Wiley & Sons Inc.)

The *leading circle* hypothesis of reentry accounts for reentry in the absence of an anatomic obstacle [26]. Reentry follows the smallest possible circuit with tissue at the vortex remaining unexcitable (Fig. 15.10b). The propagating wave must penetrate tissue that remains relatively refractory. Thus, the circuit is much smaller than the circuit in anatomical reentry and no portion of the circuit is ever fully recovered (i.e., there is no *excitable gap*). It is unclear whether leading circle reentry is responsible for clinical arrhythmias.

Propagation of impulses in cardiac tissue is dependent on myocyte fiber orientation. Cell-to-cell communication depends primarily on gap junction proteins that are unequally distributed along the cell surface. The greater density of gap junction proteins along the longitudinal axis (as compared with the transverse axis) accounts for more rapid conduction in this direction. However, the longitudinal axis is associated with a lower safety factor of conduction (i.e., longer refractory period). The differential conduction properties in the longitudinal and transverse directions provide a substrate for *anisotropic* reentry. Anisotropy may account in part for some arrhythmias in the atria, AV node, and the peri-infarct regions of myocardium [28].

Figure-eight reentry may be considered an "extension" of leading circle reentry (that also incorporates anatomic reentry and anisotropic conduction properties), in which two reentrant circuits rotate in opposite directions in close proximity to one another utilizing a central common pathway (Fig. 15.10c). This mechanism may underlie sustained monomorphic ventricular tachycardia observed in some patients with ischemic heart disease. Unlike other forms of functional reentry, figure-of-eight reentry depends on a central common pathway between the rotating reentrant waves that is delimited by unexcitable tissue. Disruption of this central pathway effectively terminates reentry.

Spiral waves represent the most complex form of functional reentry and are believed to be a possible underlying mechanism for some forms of atrial and ventricular fibrillation (Fig. 15.11). In its simplest form, spiral wave reentry may be depicted as a broken wave front that curls at its broken end and begins to rotate (Fig. 15.12) [26]. The wave propagates through cardiac muscle but is interrupted by an obstacle such as a scar. When the obstacle causes a break in the wave front, several outcomes are possible depending on the excitability of the tissue. When excitability is high after passing the obstacle, the broken ends will fuse rapidly. When excitability is lower, the broken ends cannot fuse but begin to spiral. The trajectory of each point on the wave varies according to the

curvature of the wave: the greater the curvature, the slower the conduction velocity. The variable excitability of cardiac muscle compounds the complexity of propagation. When excitability of the tissue is further reduced, propagation of the wave front is extinguished.

Finally, reentry may occur in a linear circuit in the absence of even a functional loop (Fig. 15.13). An example of this form of reentry, termed *reflection*, may be seen when local injury occurs over a short portion of the His–Purkinje fibers. In this model, reentry occurs over a single pathway and depends on the presence of a region of severely impaired (but not blocked) conduction [26]. The impulse propagates toward the region of depressed conduction, but the damaged cells are incapable of being excited and the action potential is unable to propagate further. However, a small current is generated across these cells, and if the distance across the gap is relatively small, current may reach the distal segment and bring those cells to threshold, where propagation of an action potential can be initiated. If there is sufficient delay in propagation of the current to the distal side of the gap, the distal action potential may be reflected backward across the gap, reinitiating (or reflecting) an action potential.

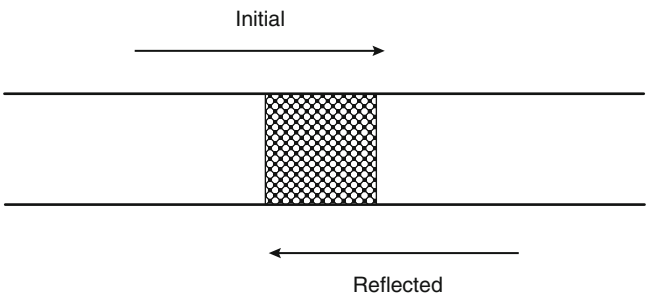

Fig. 15.13 Model of reflection. *See* text for explanation (Reprinted from Jalife et al. [26]. With permission from John Wiley & Sons Inc.)

Clinical Correlates

Most clinical supraventricular and ventricular arrhythmias are due to reentry. In this section, we describe the most common reentrant arrhythmias. The surface electrocardiogram (ECG) provides important clues to the mechanism of reentrant tachycardias (Fig. 15.14). Supraventricular tachycardias due to AV node reentry or an accessory AV pathway will typically have a short RP' interval (i.e., the interval between the P wave on surface ECG and the preceding R wave, denoted as the RP' interval <50 % of the RR interval). Conversely, supraventricular tachycardias such as atrial tachycardias, the atypical form of AV node reentry (discussed below), and the permanent form of junctional reciprocating tachycardia (a reentrant SVT due to a slowly conducting retrograde accessory pathway) typically demonstrate a long RP' interval (<50 % of the RR interval). When evaluating wide complex tachycardia, dissociation of the surface ECG P waves from the QRS complexes supports the diagnosis of ventricular tachycardia (Fig. 15.15). However, a 1:1 relationship between the P waves and QRS complexes may be observed in ventricular tachycardia (with 1:1 retrograde ventricular-to-atrial conduction) or supraventricular tachycardia conducted with a wide QRS complex.

Intra-Atrial Reentry

Intra-atrial reentrant tachycardias comprise a diverse group of arrhythmias. Reentrant arrhythmias may occur anywhere

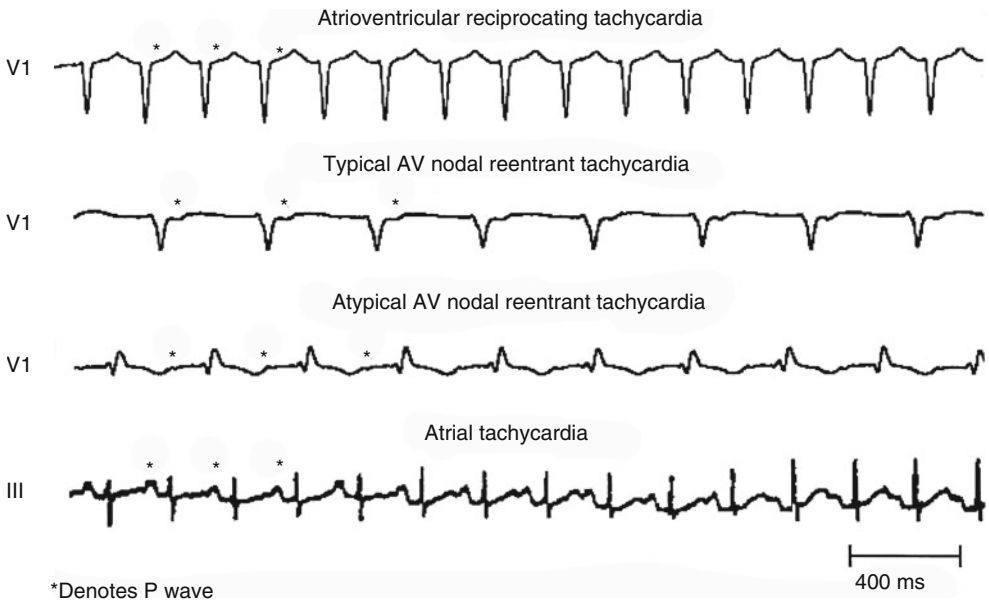

Fig. 15.14 Typical AV nodal reentrant tachycardia demonstrates a short RP' interval on the surface ECG. Similarly, orthodromic atrioventricular reciprocating tachycardia is characterized by a short RP' interval. Atrial tachycardias and atypical AV nodal reentrant tachycardia are characterized by a long RP' interval

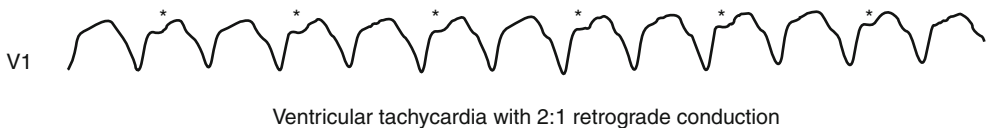

Fig. 15.15 Dissociation of the P waves (denoted with an asterisk, *) from the QRS complexes, or variable retrograde conduction to the atria, strongly supports the diagnostic of ventricular tachycardia. This is demonstrated in the figure. However, a 1:1 relationship of P waves to QRS complexes during a wide complex tachycardia may be due to either ventricular tachycardia with 1:1 retrograde conduction to the atria or a supraventricular tachycardia with 1:1 anterograde conduction to the ventricles in a patient with a preexisting bundle branch block

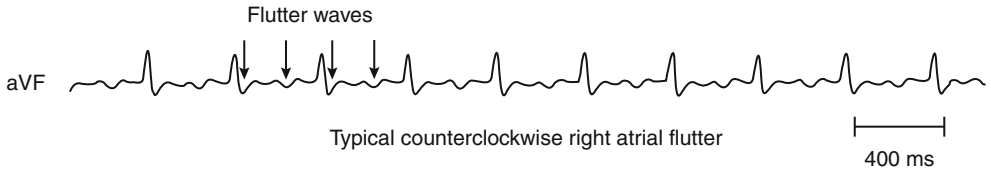

Fig. 15.16 Typical counterclockwise right atrial flutter is often characterized by 2:1 ventricular response and a ventricular rate of 150 beats per minute. Flutter waves on the surface ECG are usually negative in the inferior leads (II, III, aVF), as atrial activation proceeds down the right atrial free wall and up the interatrial septum, activating the interatrial septum and left atrium in a caudal to cranial sequence

in the atria and may affect persons with or without structural heart disease. Because areas of scar tissue typically provide the substrate for reentry, these tachycardias have been called *incisional reentrant tachycardias* [29]. Another common form of intra-atrial reentry is atrial flutter (Fig. 15.16). The "typical" form of atrial flutter occurs at a remarkably consistent rate of 250–300 beats per minute with propagation in counterclockwise fashion around the tricuspid valve annulus, down the free wall of the right atrium, and up the interatrial septum. When conduction proceeds up the interatrial septum, the caudal–cranial activation inscribes the superiorly directed flutter waves (i.e., negative in the inferior leads) observed on the surface ECG. Clockwise right atrial flutter (in the opposite direction) is less common.

Most intra-atrial reentrant tachycardias are not responsive to adenosine, β-blockers, or calcium channel blockers [5]. Over the past decade, electrophysiologists have made substantial progress in mapping and ablating reentrant atrial tachycardias. As with all reentrant arrhythmias, disruption of any part of the circuit will terminate tachycardia. For example, both the typical and atypical forms of flutter depend on a critical isthmus of conduction at the base of the right atrium. Creating a linear ablation lesion extending from the tricuspid valve annulus to the inferior vena cava blocks conduction across this isthmus and effectively eliminates tachycardia.

Atrioventricular (AV) Nodal Reentrant Tachycardia

Excluding atrial flutter and fibrillation, typical AV nodal reentrant tachycardia is the single most common form of supraventricular tachycardia and accounts for nearly 50–60 % of all sustained SVTs in adults [30, 31]. Usually, it presents

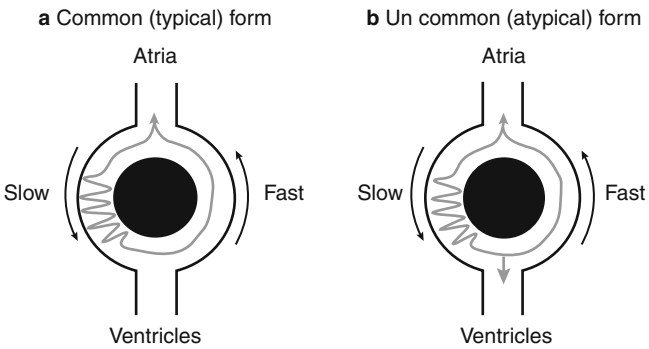

Fig. 15.17 Schematic drawings of AV nodal reentrant tachycardia. Illustrations depict two forms of supraventricular tachycardia due to reentry within the AV node, i.e., typical (**a**) and atypical forms (**b**)

before age 40, with rates typically ranging from 160 to 200 beats per minute but may vary (from 100 to 300 beats per minute). The reentrant circuit is limited to the peri-AV nodal region, with anterograde conduction proceeding over a "slow" pathway and retrograde conduction traversing a "fast" pathway [32]. In the usual case, the fast pathway has a longer refractory period than the slow pathway. Therefore, initiation of reentry occurs when a premature atrial beat blocks in the fast pathway and is conducted over the slow pathway. By the time the impulse reaches the distal portion of the slow pathway, the retrograde fast pathway has regained excitability and is able to conduct the impulse to the atrium, perpetuating the arrhythmia by engaging and activating the slow anterograde pathway. The atypical form of AV nodal reentry activates these limbs in the opposite direction; anterograde conduction proceeds over the fast pathway and retrograde conduction across the slow pathway (Fig. 15.17). As one would predict, the typical form of AV nodal reentry (with retrograde conduction up the fast pathway) is characterized by a short RP'

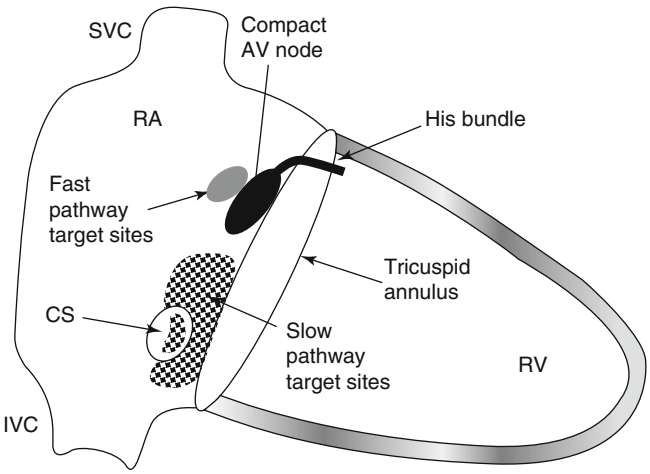

Fig. 15.18 Anatomical positions of slow and fast pathways. The posterior location of the "slow" pathway, remote from the compact AV node, makes it the target of choice for radiofrequency catheter ablation (Reprinted from Kalbfleisch and Morady [36]. With permission from Elsevier)

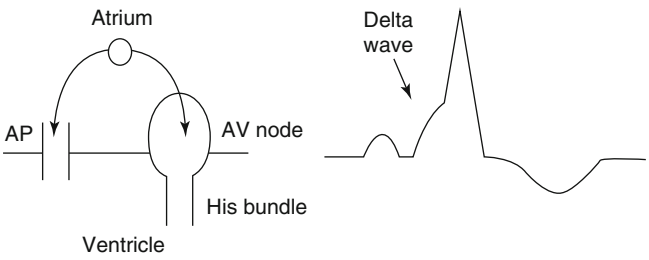

Fig. 15.19 Schematic of Wolff–Parkinson–White syndrome during normal sinus rhythm. Conduction over the accessory pathway (*AP*) activates the ventricle simultaneously with conduction over the AV node. Preexcitation of the ventricles by the accessory pathway creates the delta wave visible on the surface ECG

interval on the surface ECG, while atypical AV nodal reentry inscribes a long RP' interval. An electrophysiologic hallmark of AV nodal reentry is that neither the atria nor ventricles are necessary parts of the reentrant circuit.

Adenosine is effective in terminating reentrant tachycardias that involve the AV node and is mediated by activation of the outward potassium current $I_{K(Ado,\ ACh)}$, which hyperpolarizes the AV node to about −90 mV and abbreviates the action potential. Adenosine can terminate tachycardia in either limb, but it occurs most often in the slow pathway [33, 34]. Vagal maneuvers (carotid sinus massage or Valsalva) also terminate AV nodal-dependent reentry by activating the same outward potassium current $I_{K(Ado,\ ACh)}$.

The slow pathway is located in the region of the posteroseptal space of the interatrial septum and is readily amenable to ablation (>95 % success rate; Fig. 15.18) [35, 36]. This location, remote from the compact AV node, minimizes the chance of AV node damage during ablation. Ablation of the fast pathway also effectively treats AV nodal reentry but carries a relatively high risk of complete heart block.

Atrioventricular Reciprocating Tachycardia

Reentrant arrhythmias utilizing an accessory AV connection comprise the second most common form of regular narrow complex tachycardias (approximately 35 % of SVTs). Accessory pathways are composed of muscular bridges along the tricuspid and mitral valve annuli that provide an abnormal electrical connection between the atria and ventricles. The electrophysiologic properties of most accessory pathways resemble those of normal atrial tissue. Because the resting membrane potential is approximately −90 mV, typically, accessory pathways are insensitive to vagal maneuvers, adenosine, and Ca^{2+} channel blockers.

Most accessory pathways conduct only in one direction—retrogradely from the ventricles to the atria—and are therefore concealed during sinus rhythm. Conversely, accessory pathways with anterograde conduction properties usually result in ventricular preexcitation (known as Wolff–Parkinson–White syndrome). During sinus rhythm, conduction proceeds simultaneously down the AV node and accessory pathway (Fig. 15.19). Preexcitation of the ventricles by the accessory pathway inscribes a delta wave visible on the surface ECG that prolongs the QRS complex. Typically, the PR interval is abbreviated (<120 ms) owing to rapid conduction over the accessory pathway. Orthodromic reciprocating tachycardia (anterograde conduction over the AV node and retrograde conduction across the accessory pathway) accounts for 90 % of reentrant arrhythmias in patients with Wolff–Parkinson–White syndrome. This arrhythmia may degenerate into atrial fibrillation, which may precipitate ventricular fibrillation because of rapid conduction over the accessory pathway. A less common arrhythmia, antidromic reciprocating tachycardia (the anterograde limb being the accessory pathway and the retrograde limb being the AV node), is a regular rhythm and inscribes a wide QRS complex on the surface ECG.

Ventricular Reentrant Arrhythmias

Most ventricular arrhythmias occur in patients with a prior history of myocardial infarction. Experimental evidence suggests that mechanism of the tachycardia may be dependent on the time of the infarct. Within the first 30–60 min (early phase) following an acute myocardial infarction, the intracellular and extracellular milieux appear to favor reentrant ventricular arrhythmias, as does autonomic tone [37]. Automatic idioventricular rhythms, with rates typically between 60 and 120 beats per minute, are usually observed within the first 6–10 h (delayed phase). After the relatively quiescent second phase, the third and final stage of ventricular arrhythmias (late phase) begins within 48–72 h after infarct and is characterized by rapid monomorphic tachycardias, owing to reentry arising in the peri-infarct border zone. Inhomogeneous conduction properties of the peri-infarction tissue create regions of slow and rapid conduction, causing anisotropic and figure-of-eight reentry. The risk of reentrant late-phase ventricular arrhythmias persists indefinitely following myocardial infarction and is thought to account for at least half of all deaths among myocardial infarction survivors. Electrophysiologic studies and endocardial mapping in humans have demonstrated that monomorphic VT that occurs late after a myocardial infarction is caused by areas of slow conduction and diastolic activation. These arrhythmias may be induced or terminated with pacing maneuvers.

Another example of reentrant ventricular tachycardia occurring in patients with heart disease is bundle branch reentrant VT. This example of anatomic reentry is usually observed in patients with diseased His–Purkinje system function, complete or incomplete left bundle branch block during sinus rhythm, and a nonischemic dilated cardiomyopathy. The incidence of bundle branch reentry as the cause of sustained monomorphic ventricular tachycardia ranges from less than 1 to 6 % [38]; this form of VT most often has a left bundle branch block, left superior axis morphology. It is typically initiated by a ventricular premature beat that follows a pause. The premature impulse blocks in the retrograde direction within the right bundle but conducts transseptally to retrogradely activate the left bundle. When the impulse reaches the His bundle, it is able to engage the right bundle in the anterograde direction and then continues back to the left bundle (Fig. 15.20). It is important to recognize this form of tachycardia since it is readily curable by radiofrequency catheter ablation of the right bundle.

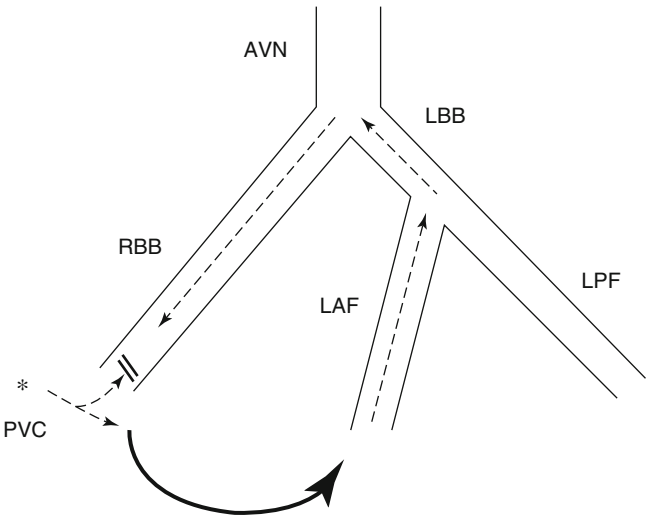

Fig. 15.20 Bundle branch reentry circuit, utilizing the left anterior fascicle (*LAF*) as the retrograde limb of the circuit and the right bundle branch (*RBB*) as the anterograde limb. *AVN* atrioventricular node, *LAF* left anterior fascicle, *LBB* left bundle branch, *LPF* left posterior fascicle, *PVC* premature ventricular complex, *RBB* right bundle branch Asterisk (*) denotes PVC origin

Functional reentry may be responsible for the initiation of ventricular arrhythmias in patients with Brugada syndrome, although some data suggest an alternative mechanism [39]. These patients, first described in 1992 [40], present with an ECG pattern of right bundle branch block, right precordial downsloping ST segment elevation (leads V1–V3) with a normal QTc interval, and have no evidence of structural heart disease. ST segment elevation is due to relatively early epicardial repolarization with respect to the endocardium and results from greater expression I_{to} and I_{ks} in the epicardium. There is evidence that Brugada syndrome is a primary electrical disease, and in some families it has been linked to mutations causing loss of function in a sodium channel (SCN5A) [41]. This results in an outward shift of the balance of current at the end of phase 1 of the action potential, leading to the loss of the action potential dome, preferentially in the epicardial layer. The subsequent abbreviation of the action potential at some epicardial sites leads to the substrate for phase 2 reentry. Phase 2 reentry has been studied in a canine model of simulated ischemia, where loss of epicardial action potential dome (after exposure to a K^+ channel opener) gives rise to ST-segment elevation (Fig. 15.21) [42].

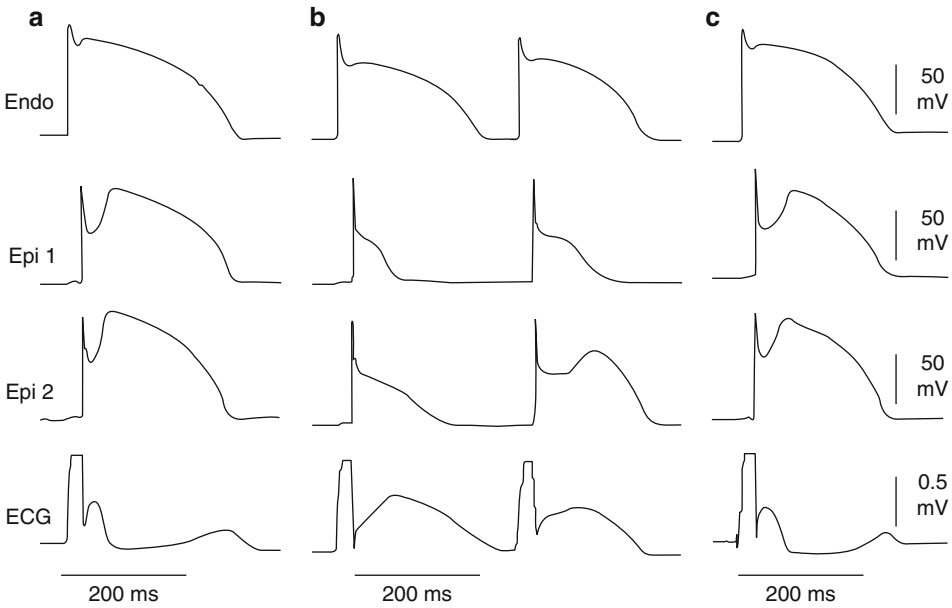

Fig. 15.21 Loss of epicardial AP dome after exposure to K^+ channel opener gives rise to ST-segment elevation in arterially perfused RV wedge preparation. (**a**) Control. (**b**) Pinacidil (causes loss of action potential dome in epicardium and marked abbreviation of the action potential duration, resulting in a transmural voltage gradient). (**c**) Recorded 2 min later in continued presence of pinacidil. *Endo* endocardial layer, *Epi* epicardial layer(s). *ECG* electrocardiogram (Reprinted from Yan and Antzelevitch [42]. With permission from Lippincott Williams & Wilkins)

References

1. Ackerman MJ, Clapham DE. Ion channels—basic science and clinical disease. N Engl J Med. 1997;336:1575–86.
2. Ackerman MJ, Clapham DE. Normal cardiac electrophysiology. In: Chien K, editor. Molecular basis of cardiovascular disease. Philadelphia: W. B. Saunders; 1999. p. 281–301.
3. Surawicz B. Normal and abnormal automaticity. In: Rosen MR, Janse MJ, Wit AL, editors. Cardiac electrophysiology: a textbook. Mount Kisco: Futura Publishing; 1990. p. 159–73.
4. Lerman BB, Stein KM, Markowitz SM. Adenosine-sensitive ventricular tachycardia: a conceptual approach. J Cardiovasc Electrophysiol. 1996;7:559–69.
5. Markowitz SM, Stein KM, Mittal S, et al. Differential effects of adenosine on focal and macroreentrant atrial tachycardia. J Cardiovasc Electrophysiol. 1999;10:489–502.
6. DiFrancesco D, Angoni M, Maccaferri G. The pacemaker current in cardiac cells. In: Zipes DP, Jalife J, editors. Cardiac electrophysiology: from cell to bedside. Philadelphia: W. B. Saunders; 1995. p. 96–103.
7. Lerman BB. Response of nonreentrant catecholamine-mediated ventricular tachycardia to endogenous adenosine and acetylcholine. Evidence for myocardial receptor-mediated effects. Circulation. 1993;87:382–90.
8. Schwartz PJ, Stramba-Badiale M, Crotti L, et al. Prevalence of the congenital long-QT syndrome. Circulation. 2009;120:1761–7.
9. Jervell A, Lange-Nielsen F. Congenital deaf-mutism, functional heart disease with prolongation of the QT interval, and sudden death. Am Heart J. 1957;54:59–68.
10. Romano C, Gemme G, Pongiglione R. Aritmie cardiache rare dell'eta'pediatrica. II. Accessi sincopali per fibrillazione ventricolare parossistica. Clin Pediatr (Bologna). 1963;45:656–83.
11. Ward OC. A new familial cardiac syndrome in children. J Ir Med Assoc. 1964;54:103–6.
12. Yang Y, Yang Y, Liang B, et al. Identification of a Kir3.4 mutation in congenital long QT syndrome. Am J Hum Genet. 2010;86:872–80.
13. Keating MT. The long QT syndrome: a review of recent molecular genetic and physiologic discoveries. Medicine. 1996;75:1–5.
14. Schwartz PJ, Moss AJ, Vincent GM, et al. Diagnostic criteria for the long QT syndrome. An update. Circulation. 1993;88:782–4.
15. Ackerman MJ, Priori SG, Willems S, et al. HRS/EHRA expert consensus statement on the state of genetic testing for the channelopathies and cardiomyopathies. Heart Rhythm. 2011;8:1308–39.
16. Luo CH, Rudy Y. A dynamic model of the cardiac ventricular action potential. II. Afterdepolarizations, triggered activity, and potentiation. Circ Res. 1994;74:1097–113.
17. Han X, Ferrier GR. Contribution of Na^+-Ca^{2+} exchange to stimulation of transient inward current by isoproterenol in rabbit cardiac Purkinje fibers. Circ Res. 1995;76:664–74.
18. Lerman BB, Belardinelli L, West GA, et al. Adenosine-sensitive ventricular tachycardia: evidence suggesting cyclic AMP-mediated triggered activity. Circulation. 1986;74:270–80.
19. Lerman BB, Stein K, Engelstein ED, et al. Mechanism of repetitive monomorphic ventricular tachycardia. Circulation. 1995;92:421–9.
20. Iwai S, Cantillon DJ, Kim RJ, et al. Right and left ventricular outflow tract tachycardias: evidence for a common electrophysiologic mechanism. J Cardiovasc Electrophysiol. 2006;17:1052–8.
21. Lerman BB, Stein KM, Markowitz SM. Mechanisms of idiopathic left ventricular tachycardia. J Cardiovasc Electrophysiol. 1997;8:571–83.
22. Lerman BB, Stein KM, Markowitz SM, et al. Catecholamine-facilitated reentrant ventricular tachycardia: uncoupling of adenosine's antiadrenergic effects. J Cardiovasc Electrophysiol. 1999;10:17–26.
23. Priori SG, Napolitano CN, Tiso N, et al. Mutations in the cardiac ryanodine receptor gene (hRyR2) underlie catecholaminergic polymorphic ventricular tachycardia. Circulation. 2001;103:196–200.
24. Laitinen PJ, Brown DM, Piippo K, et al. Mutations of the cardiac ryanodine receptor (RyR2) gene in familial polymorphic ventricular tachycardia. Circulation. 2001;103:485–90.
25. Laitinen PJ, Swan H, Kontula K. Molecular genetics of exercise-induced polymorphic ventricular tachycardia: identification of three novel cardiac ryanodine receptor mutations and two common calsequestrin 2 amino-acid polymorphisms. Eur J Hum Genet. 2003;11:888–91.
26. Jalife J, Delmar M, Davidenko J, et al. Basic cardiac electrophysiology for the clinician. Armonk: Futura Publishing; 1999.

27. Prystowsky EN, Klein GJ. Mechanism of tachycardia. In: Prystowsky E, Klein G, editors. Cardiac arrhythmias: an integrated approach for the clinician. New York: McGraw-Hill; 1994. p. 81–95.
28. Spach MS, Dolber PC, Heidlage JF. Influence of the passive anisotropic properties on directional differences in propagation following modification of the sodium conductance in human atrial muscle. A model of reentry based on anisotropic discontinuous propagation. Circ Res. 1988;62:811–32.
29. Lesh MD, Kalman JM. To fumble flutter or tackle "tach"? Toward updated classifiers for atrial tachyarrhythmias. J Cardiovasc Electrophysiol. 1996;7:460–6.
30. Josephson ME, Kastor JA. Supraventricular tachycardia: mechanisms and management. Ann Intern Med. 1977;87:346–58.
31. Wu D, Denes P. Mechanisms of paroxysmal supraventricular tachycardia. Arch Intern Med. 1975;135:437–42.
32. Benditt D, Reyes W, Gornick C, et al. Supraventricular tachycardias: recognition and treatment. In: Naccarelli G, editor. Cardiac arrhythmias: a practical approach. Mount Kisco: Futura; 1991. p. 135–76.
33. DiMarco JP, Sellers TD, Lerman BB, et al. Diagnostic and therapeutic use of adenosine in patients with supraventricular tachyarrhythmias. J Am Coll Cardiol. 1985;6:417–25.
34. Lerman BB, Greenberg M, Overholt ED, et al. Differential electrophysiologic properties of decremental retrograde pathways in long RP' tachycardia. Circulation. 1987;76:21–31.
35. Calkins H, Yong P, Miller JM, et al. Catheter ablation of accessory pathways, atrioventricular nodal reentrant tachycardia, and the atrioventricular junction: final results of a prospective, multicenter clinical trial. Circulation. 1999;99:262–70.
36. Kalbfleisch SJ, Morady F. Catheter ablation of atrioventricular nodal reentrant tachycardia. In: Zipes D, Jalife J, editors. Cardiac electrophysiology: from cell to bedside. Philadelphia: W. B. Saunders; 1995. p. 1477.
37. Scherlag BJ, El-Sherif N, Hope R, et al. Characterization and localization of ventricular arrhythmias resulting from myocardial ischemia and infarction. Circ Res. 1974;35:372–83.
38. Caceres J, Jazayeri M, McKinnie J, et al. Sustained bundle branch reentry as a mechanism of clinical tachycardia. Circulation. 1989;79:256–70.
39. Nademanee K, Veerakul G, Chandanamattha P, Chaothawee L, Ariyachaipanich A, Jirasirirojanakorn K, et al. Prevention of ventricular fibrillation episodes in Brugada syndrome by catheter ablation over the anterior right ventricular outflow tract epicardium. Circulation. 2011;123:1270–12709.
40. Brugada P, Brugada J. Right bundle branch block, persistent ST segment elevation and sudden cardiac death: a distinct clinical and electrocardiographic syndrome. J Am Coll Cardiol. 1992;20:1391–6.
41. Chen Q, Kirsch G, Zhang D, et al. Genetic basis and molecular mechanism for idiopathic ventricular fibrillation. Nature. 1998;392:293–6.
42. Yan G, Antzelevitch C. Cellular basis for the Brugada syndrome and other mechanisms of arrhythmogenesis associated with ST-segment elevation. Circulation. 1999;100:1660–6.

Recommended Reading

Ackerman MJ, Priori SG, Willems S, et al. HRS/EHRA expert consensus statement on the state of genetic testing for the channelopathies and cardiomyopathies. Heart Rhythm. 2011;8:1308–39.
Jalife J, Delmar M, Davidenko J, et al. Basic cardiac electrophysiology for the clinician. Armonk: Futura Publishing; 1999.
Lerman BB, Stein KM, Markowitz SM, et al. Ventricular arrhythmias in normal hearts. Cardiol Clin. 2000;18:265–91.
Priori SG, Napolitano CN, Tiso N, et al. Mutations in the cardiac ryanodine receptor gene (hRyR2) underlie catecholaminergic polymorphic ventricular tachycardia. Circulation. 2001;103:196–200.
Yan G, Antzelevitch C. Cellular basis for the Brugada syndrome and other mechanisms of arrhythmogenesis associated with ST-segment elevation. Circulation. 1999;100:1660–6.